MICROMACHINED STIMULATING ELECTRODES

Quarterly Report #1

(Contract NIH-NINDS-N01-NS-2-2379)

October - December 1992

Submitted to the

Neural Prosthesis Program
National Institute of Neurological Disorders and Stroke
National Institutes of Health

by the

Solid-State Electronics Laboratory
Bioelectrical Sciences Laboratory
Department of Electrical Engineering and Computer Science
University of Michigan
Ann Arbor, Michigan
48109-2122

February 1993

MICROMACHINED STIMULATING ELECTRODES

Summary

During the past quarter, research performed under this program has focused on four primary areas. Passive probes have been fabricated having multiple shanks and site areas ranging from 400μm^2 to 1600μm^2 so that the problems associated with tissue access resistance and the physiological effects of stimulation can be studied chronically. A series of passive probes is also being designed to allow different tip shapes to be created so that the tips can be optimized to obtain minimum insertion force and minimum tissue damage. A combined stimulation-recording probe is also in development that should allow questions regarding the fall-off of spike amplitudes observed with chronic recording electrodes after 8-10 months in-vivo to be answered.

While the new process for active probes has produced good results and appears to have solved the former processing problems associated with circuit interconnect and encapsulation, several minor problems still needing correction have been identified. The perimeter of these probes needs to be expanded near the outer corners of the circuit area to prevent undercutting during the silicon etch used to separate the probes from the wafer; a process has also been identified for further sharpening the probe tips using a shallow boron diffusion to extend the substrate beyond that produced using the deep etch-stop diffusion. In addition, experiments to better characterize appropriate dielectric thicknesses on the probe shanks to prevent bowing have been carried out. This reoptimization has been motivated by the retention of low-temperature oxide (LTO) on the shanks of some of our recent probes. Finally, excessive low-voltage leakage has been seen on the recently-fabricated active stimulating probes. We suspect this may be due to punchthrough of the epitaxial region. Studies are underway to confirm this cause, in which case the epitaxial layer thickness will be increased somewhat on future fabrication runs.

The design of the circuitry for a second-generation active probe, STIM-2, was completed during the past term. This probe will be implemented in 8- and 16-shank versions and will feature eight parallel channels. Per-channel currents will be controlled within 1μA over a range from 0 to $\pm$127μA. A front-end selector will interface eight DACs to 8 sites from among 64 present on the probe, thus allowing precise positioning of the active sites in tissue. The timing and data protocols developed for STIM-2 allow all modes developed for STIM-1 to be retained. In addition, additional modes such as the ability to record from any site have been added. The circuitry allows direct addressing of up to 64 sites with a single 16-bit data word and using a second 16-bit word allows up to 256 such probes to be addressed. Hence, normal operations on a single probe can be carried out using single 16-bit instructions with a 4μsec time period between changes in probe state using a 4.5MHz clock. Switching between probes as well as the implementation of modes insensitive to speed (e.g., current calibration, site testing) use the slower 32-bit instructions. Progress has also been made with the external system for use with these active probes in both the hardware and software areas. This system will be used in the further testing of both STIM-1 and STIM-2.

During the coming quarter, we hope to begin a series of chronic stimulation experiments to explore the effects of stimulation on the tissue. We also hope to complete the development of the electrodes needed for the penetration studies. The testing of STIM-1 should be completed along with any appropriate design optimizations. Finally, we hope to receive MOSIS chips back with the circuitry for STIM-2 so that this circuitry can be tested to establish design validity. Following that, a new fabrication run of both STIM-1 and STIM-2 will be initiated.

MICROMACHINED STIMULATING ELECTRODES

1. Introduction

The goal of this research is the development of active multichannel arrays of stimulating electrodes suitable for studies of neural information processing at the cellular level and for a variety of closed-loop neural prostheses. The probes should be able to enter neural tissue with minimal disturbance to the neural networks there and deliver highly-controlled (spatially and temporally) charge waveforms to the tissue on a chronic basis. The probes consist of several thin-film conductors supported on a micromachined silicon substrate and insulated from it and from the surrounding electrolyte by silicon dioxide and silicon nitride dielectric films. The stimulating sites are activated iridium, defined photolithographically using a lift-off process. Passive probes having a variety of site sizes and shank configurations have been fabricated successfully and distributed to a number of research organizations nationally for evaluation in many different research preparations. For chronic use, the biggest problem associated with these passive probes concerns their leads, which must interface the probe to the outside world. Even using silicon-substrate ribbon cables, the number of allowable interconnects is necessarily limited, and yet a great many stimulating sites are ultimately desirable in order to achieve high spatial localization of the stimulus currents.

The integration of signal processing electronics on the rear of the probe substrate (creating an "active" probe) allows the use of serial digital input data which can be demultiplexed onto the probe to provide access to a large number of stimulating sites. Our goal in this area of the program has been to develop a family of 16-site active probes capable of chronic implantation in tissue. For such probes, the digital input data must be translated on the probe into per-channel current amplitudes which are then applied to the tissue through the sites. Such probes require five external leads, virtually independent of the number of sites used. As discussed in our previous reports, we have defined three probes which represent the first-generation of these active stimulating devices and have designated them as STIM-1, -1a, and -1b. All three probes provide 8-bit resolution in setting the per-channel current amplitudes over the biphasic range from 2μA to ±254μA; however, the probes differ markedly in the number of sites that can be active at any one time. STIM-1 offers the ability to utilize all 16 sites independently and in parallel, while -1a allows only two sites to be active at a time (bipolar operation), and -1b is a monopolar probe, allowing the user to guide an externally-provided current to the site selected by the digital address. The circuit complexity among these designs spans an order of magnitude in device count, ranging from a 400 transistors (STIM-1b) to over 7000 transistors (STIM-1). The high-end STIM-1 contains provisions for numerous saftey checks and for features such as remote impedance testing in addition to its normal operating modes.

During the past quarter, research on this contract has focused on several areas. New multisite multishank passive probes have been realized for studying access resistance and associated IR drops during chronic stimulation as well as questions regarding the physiological effects of chronic stimulation. A series of passive probes are also being designed in order to explore the optimization of tip shape for minimum-force penetration of

membranes such as pia arachnoid and minimum tissue damage. Several problems associated with the first-generation active probes (STIM-1) have been identified and solutions found, and the design of STIM-2 has been nearly completed. These activities are described in the sections below.

2. *Passive Stimulating Electrode Development*

Two new passive stimulating probe designs were included on the recently-run "Heater" mask set. As discussed in the last quarterly report, we are planning to do *in-vivo* studies to gather additional data on the access voltage (IR drop) developed between a driven site and tissue ground. Up until this point, we have had only one stimulating probe design with an integrated silicon cable, and this probe had very large (4000μm^2) sites. The new design to be used for the IR drop studies is shown in Fig. 1. This probe has four shanks, each of which houses a pair of sites of various sizes (400, 800, 1200 and 1600μm^2). The site and shank separations are 200μm. The integrated ribbon cable will give us the ability to perform chronic stimulation experiments in which the effects on tissue of varying IR drops can be studied.

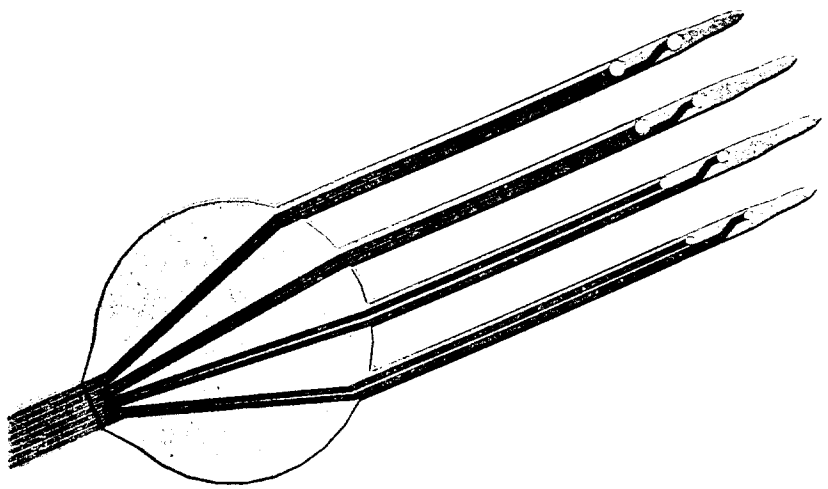

Fig. 1: A four-shank stimulating probe with four bipolar electrode pairs to be used for studies of access resistance and IR drop in chronic preparations.

The second new passive stimulating probe design is shown in Fig. 2. This probe has three shanks, each with a pair of 1000μm^2 sites. The site and shank separations here are again 200μm. These probes will be used to determine how site-site impedance, thresholds, stimulus-response curves and IR drop vary under conditions of stimulation and with placement of the sites on the probe substrate. Each of these measurements will be

Good - we need to [illegible]

taken for sites both along the shank and between shanks. Bipolar stimulation will be performed for 20 hours on a given animal using sites both along the shank and between shanks (for instance, in Fig. 3, between sites 1 and 2 and between sites 4 and 6). The possible formation of a fluid capsule around the shanks and the eventual development of gliosis may cause the measured properties to differ for the two different cases (i.e., along vs. between shanks). Experiments will provide several time series of measurements which can be used to infer these properties.

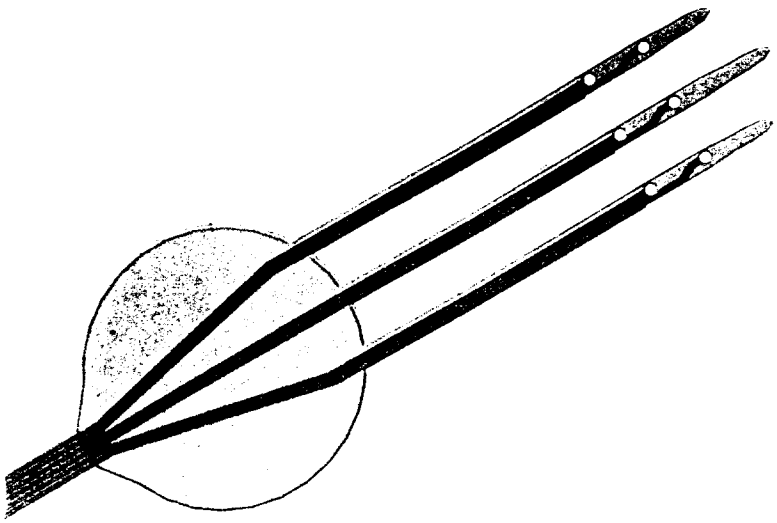

Fig. 2: A three-shank stimulating probe for use in chronic preparations.

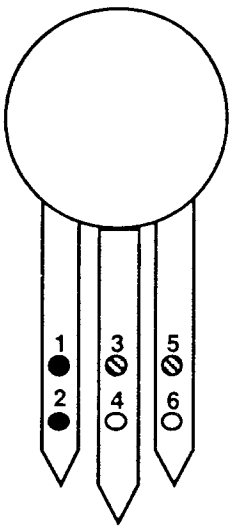

Fig. 3: Schematic of the bipolar site pairs for the probe shown in Fig. 2.

For these studies, the probe will be implanted in guinea pig CN and a recording wire will be placed in brachium of the IC to record evoked potentials. Intraoperative stimulation and recording will be performed to optimize placement. Stimulus-response and impedance data will be taken immediately post-operative and then the animal will be permitted to recover for 10 days. On the eleventh day, the daily stimulation protocol will be initiated. A given day will begin with the standard measurements (impedance, stimulus-response curves and IR drop for bipolar sites both along and between shanks). The awake, restrained animal will then be subjected to 20 hours of stimulation (4 hours per day for 5 days) at a given intensity. The stimuli will be charge balanced pulses, 200μsec per phase, delivered at a frequency of 100 Hz. Three to four animals will be used for each stimulus intensity. It is anticipated that the lowest intensity to be used will be 25μA. The highest intensity will be 150μA, the upper safe limit for a 1000μm^2 site as set by the water window. Several median intensities will also be used. The standard measurements will be taken at the end of each stimulation period. The animal will survive for 4 weeks after the conclusion of the stimulation protocol and will then be euthanized for histology. Quantitative studies on cell populations as a function of time and spatial distribution will be accomplished. These studies should also yield information on tissue damage as a function of stimulus intensity.

3. Penetration Studies

During the past quarter, preparations have been made for a study in probe tip optimization for penetration of membranes such as the dura and the pia arachnoid. The criterion for an optimal probe tip are that the shape should allow ease of penetration with minimal dimpling of the cortical surface, minimize tissue damage and reaction along the track, and permit a high degree of probe-tissue coupling for effective recording and stimulation. The tips shown in Fig. 4 illustrate the basic geometries that will be studied as realized using combinations of (nearly) isotropic boron diffusion, wet silicon etching in EDP, and selective dry etching. The wet etch will stop when the boron concentration in the silicon substrate exceeds about 5 x $10^{19}cm^{-3}$, whereas the dry etches are largely insensitive to doping. The simple diffused tip shown in the upper left in the figure results from diffusion only and is rather blunt and rounded. In contrast, when the boron diffusion is allowed to be much wider than the intended probe, anisotropic RIE-based dry etching can be used to slice through this layer resulting in a probe of nearly constant thickness and a rather chisel-shaped profile as in the upper right. RIE can also be used to produce sloped sidewalls. Finally, as shown at the bottom in Fig. 4, the boron etch-stop can be combined with RIE to produce a more needle-shaped tip. Here, the tip narrows sufficiently that the boron diffusion transistions from a full area source to a line source, with a corresponding decrease in the diffusion depth as we approach the tip. The effect is to markedly taper the silicon substrate depth as we approach the tip after EDP etching. RIE can still be used on the sidewalls to decrease their rounding or the rounding there can be retained. This approach probably will result in the sharpest tips and those most capable of membrane penetration.

Several different tip angles of each of these basic shapes will be fabricated on both single- and multi-shank probes. The probes will include strain gauges at the bases of the shanks to measure the penetration force. They will also contain four-electrode structures for monitoring the tissue resistivity near the probe shank in hopes of obtaining some

indication of the tissue damage being created by the insertion process. Hence, we should have reliable measurements on penetration force and cortical dimpling as a function of tip shape and perhaps some measure of tissue damage as well. The probe insertions will also be documented with video-equipped dissection microscopes. These probes are currently in layout and we hope to begin fabrication during the coming quarter.

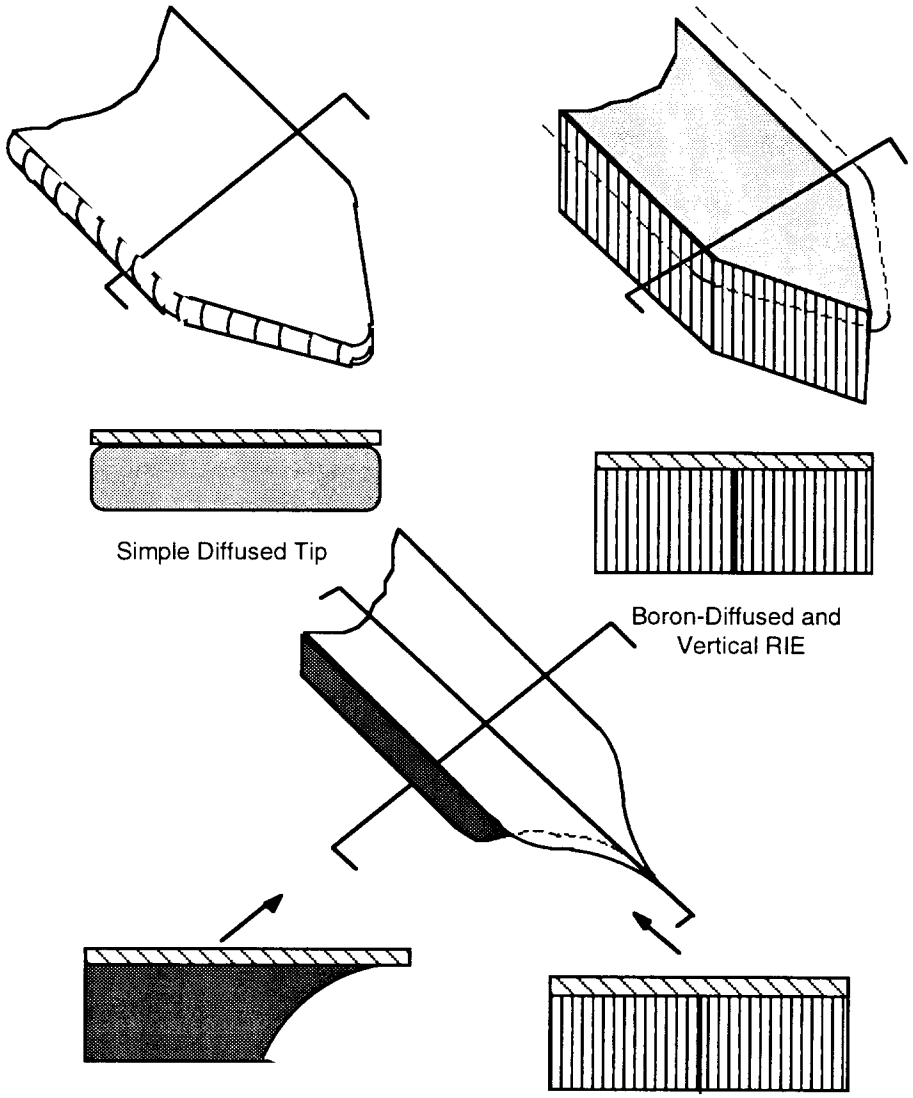

Fig. 4: Tip geometries realizable using combinations of boron-diffused etch-stops, wet etching of the silicon substrate in EDP, and dry etching using RIE.

Preparations have also been made for a chronic study in which stimulation may help in determining the cause of the decreased neural activity noted around chronic recording probes after 8-10 months of implantation. It is not clear at this time whether this decreased

activity is due to an actual decline of activity in the tissue or whether the sites are no longer effectively coupling to the associated ionic currents, e.g., due to tissue buildup adjacent to the sites. Multi-shank probes with combinations of stimulation and recording sites will be implanted chronically in laboratory animals. Figure 5 shows an example of the probes to be used. They consist of three shanks. The outer shanks contain two stimulating sites each, while the center shank has several recording sites. The recording ability of these sites will be assessed periodically throughout the life of the implant. The ability of the sites to record the tissue potentials caused by stimulating along the adjacent shanks and across (between) them will also be monitored. If the single-unit recording ability of the probe appears to decline, the stimulation sites should provide an indication of whether this is due to actual decreased activity (since the activity of the artificial "neurons" generated via the stimulating sites is known) or whether it is due to encapsulation or some other effect. This experiment will make use of, and depend on, the extremely low on-chip crosstalk on these probe structures. These probes are also in layout and are expected to be fabricated during the coming quarter.

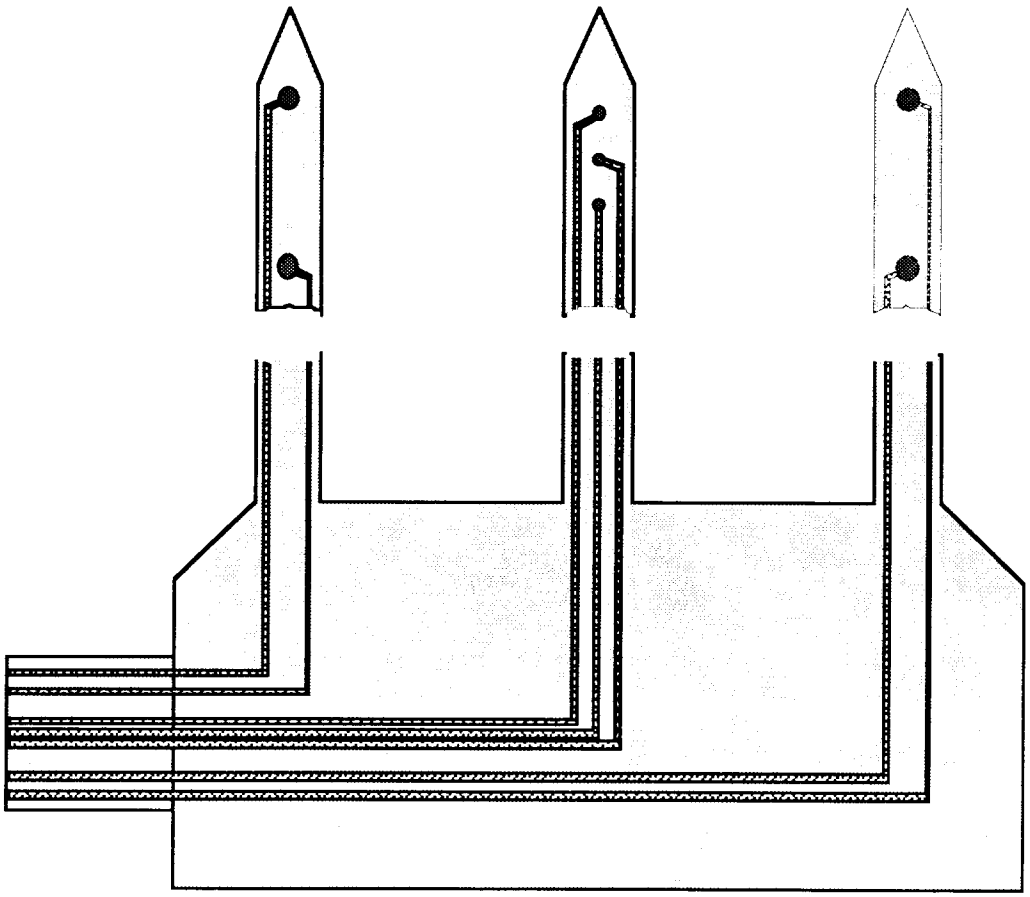

Fig. 5: Top view of a multishank probe containing stimulating and recording sites and intended for chronic studies of electrode-cell coupling.

4. *Development of Active Stimulating Probes*

As discussed in previous quarterly reports, the circuitry for our first-generation active stimulating probes (STIM-1, -1a, -1b) has been fully verified via simulation and via fabrication in a commercial foundry (MOSIS). This circuitry meets all of the design goals for such circuits, offering 16-channels of stimulation with 8-bit resolution in current over a range from zero to ±254μA. The circuits run from a 4MHz clock, allowing the current on any channel to be altered within 4μsec, which is fast enough to be virtually simultaneous to the tissue. The processing problems associated with integrating this circuitry onto probes have been solved with the use of aluminum circuit interconnect with an overlayer of low-temperature oxide (LTO). In chronic use this would typically be covered by PECVD nitride, by a metal shield layer, and by a polymer. These would act as additional chemical barriers and as an optical shield. Probes have been implemented in monopolar, bipolar, and fully-parallel designs. Tests on these three probe types have shown them to be functional at low voltage, but have also revealed several minor problems that must still be corrected. These problems are the following:

1) *Edge Undercutting*: The EDP silicon etch undercuts the boron-diffused perimeter of the probes sufficiently that the lightly doped material in the circuit area is attacked near the probe corners. This caused a substantial yield loss on the last process run.

2) *Tip Sharpness*: The probe tips need to be made sharper to more easily penetrate the brain.

3) *Probe Flatness*: The stress balance between the substrate and the probe dielectrics needs to be fine-tuned to produce probes that do not bow when released from the wafer. This bowing has been noticeable with the addition of LTO to the process.

4) *Voltage Limitations*: The present STIM-1 probes appear to function acceptably at low voltage (±3V) but do not work at higher voltages and draw excessive current. This appears to be due to punchthrough between the p-wells and the substrate across the thin epi layer.

Section 4.1 below will describe work to overcome the above problems. Section 4.2 then discusses the design developed for our second-generation probe, STIM-2.

4.1 *Fine-Tuning of the STIM-1 Design*

Probe Edge Optimization

During the development of the STIM-1 probe, the major yield loss of came from the failure of the boron-doped perimeter of the active circuit area to protect that area from the silicon etch. Silicon etch-rates in EDP are highly orientation dependent. The slowest etch rate is along the <111> direction, and the fastest rate is along the <100> direction. This means that although the sides of the circuit area do not tend to undercut (with or without the boron-doped perimeter), the outside corners tend to undercut rapidly since they offer a <100> plane to the etch. Figure 6 shows a bottom view of STIM-1 near the corners of the circuit area. The etch has proceeded under the boron-doped perimeter and then upward into

the lightly doped region to remove portions of the circuitry. The circuit patterns (i.e., the remaining oxide layers, polysilicon, and metal) are clearly visible.

There are two solutions to this problem, and both are simple to implement in hindsight. The first is to simply increase the width of the perimeter so that the etch will not be able to reach the circuit area. The second is to place fillets on the outer corners to delay the etch only where needed as shown in Fig. 7. Either or both of these solutions will correct the problem. They are being implemented on a modified STIM-1 and on our second-generation active stimulating probe, STIM-2.

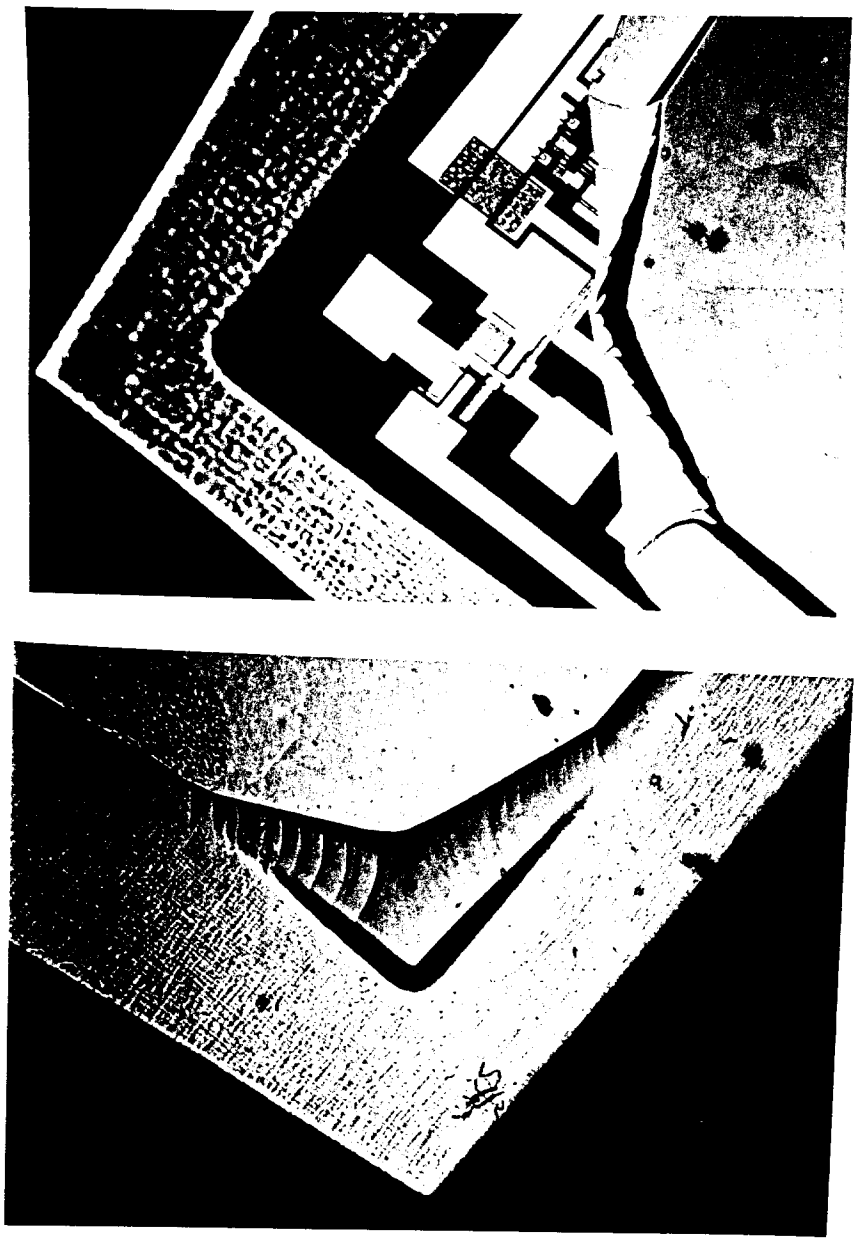

Fig. 6: Two views of the back side of active STIM-1 probes showing the excessive undercutting during the silicon etch with the associated attack of the circuit area.

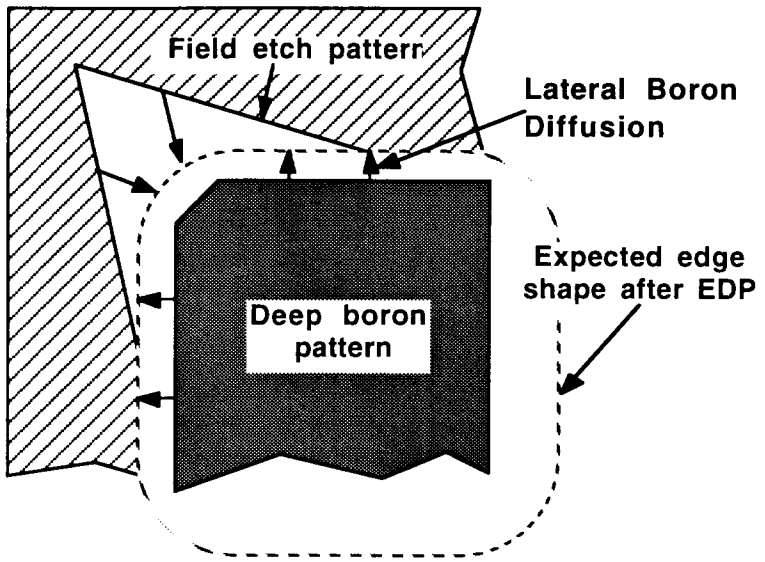

Fig. 7: Use of fillets on the outer corners of the circuit areas to delay undercutting in these regions.

Tip Sharpness

Probe tips should form tip angles of 20° or less for easy insertion and minimal tissue damage. This specification is hard to meet using only deep boron diffusion because of the large lateral diffusion during drive-in. Figure 8 shows an SEM view of a probe tip when only diffusion is used. The tip angle is about 40°. In order to achieve a sharper tip, several options can be considered as mentioned in section 3 above: 1) dry micromachining, 2) a shallow boron etch-stop process, and 3) a p^+ source/drain implantation process. Among these options, option 1 has been discussed above. Options 2 and 3 essentially involve using a second boron doping process at the tips which is much shallower than the process used on the main part of the shank and thus having much less lateral spreading. To a first approximation, the shallow diffusion of the ribbon cable process could be used, extending it somewhat beyond the tip defined by the main deep diffusion. Alternatively, option 3 could be used, employing the source/drain implant of the circuit process. Neither of these last two options require any extra masking steps when used with an active probe. Figure 9 shows how to make a sharper tip with no additional masks during the normal micromachined CMOS process. The major concept of this technique is the use of the p^+ source/drain implantation (or the shallow ribbon-cable diffusion) to extend the deep boron diffusion at the tip. This thinner layer is shallow enough that lateral diffusion is not significant and hence the final probe produced can more nearly retain the sharpness of the mask itself.

Probe Shank Optimization

The final probe shank should be straight and flat without any bending. However, bowing can sometimes occur because of stress mismatch due to the different thermal

expansion coefficients of the substrate and the various dielectric layers. To find an optimum structure for the probe shank, simulations were performed. The main purpose of these simulations was to determine the contributions to bending of the various dielectric layers and to determine their optimum thicknesses to produce a flat shank. Table 1 shows the simulation results using ANSYS, a commercial software program, to analyze the structure, while Fig. 10 shows the shank model used in these simulations.

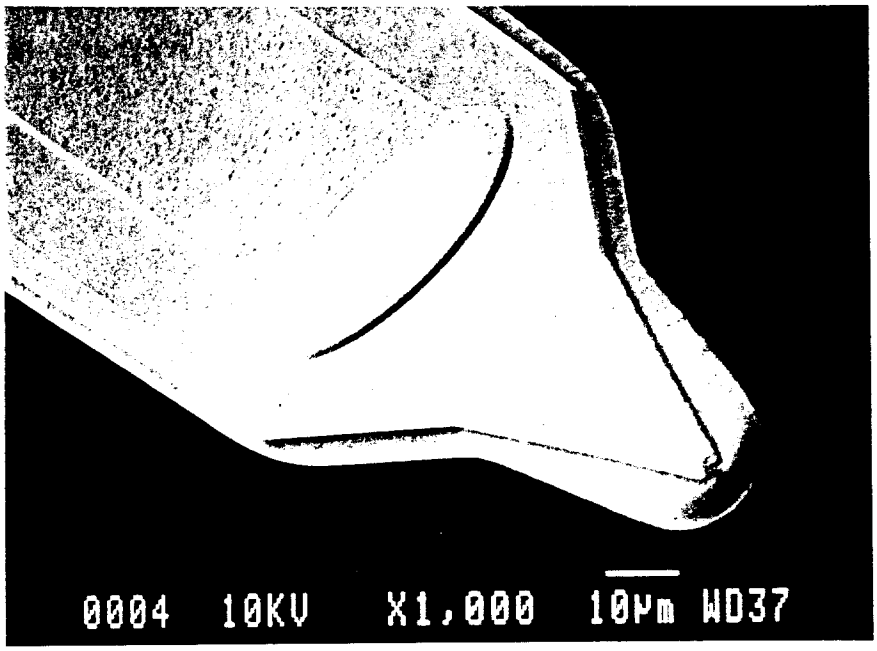

Fig. 8: SEM view of a rounded probe tip produced using only a deep boron diffusion.

Low-Voltage Limit

The source of the low limit on power supply for the present probes is still under investigation; however, since it is below 5V and is common to all probes, we feel it is most likely a process problem and not a circuit problem. This limit was not seen on the MOSIS chips. Most likely, it is related to the relatively deep p-well used in our process and is due to punchthrough between the p-well and the substrate. We will explore this in detail using the test circuits on our STIM-1 wafers. If this is the cause, the easiest solution will be to increase the epitaxial junction depth slightly and thus avoid the problem. Our recording probes are using 16µm epi instead of 10µm epi, and we do not expect them to experience this problem. The results of this investigation will be discussed in the next quarterly report.

4.2 Design of a Second-Generation Active Probe, STIM-2

During the past quarter, the design for STIM-2 has been completed. The resulting probes are now in layout. The new probe contains a number of newly designed circuits and other features, including a negative pulse detector, a clock-controlled decoder with

fewer transistors, a simple level shifter having no static power dissipation, wider lateral clearances around the p-wells to ensure freedom from lateral punchthrough, and the use of wider metal for power buses. Table 2 summarizes the specifications of this new probe. It will be implemented in both eight-shank and 16-shank versions with a front-end channel selector that will access 64 sites from 8 DACs. Thus, 8 of the 64 sites can be active simultaneously. In spite of the somewhat greater layout margins, the total circuitry will be no larger than on STIM-1.

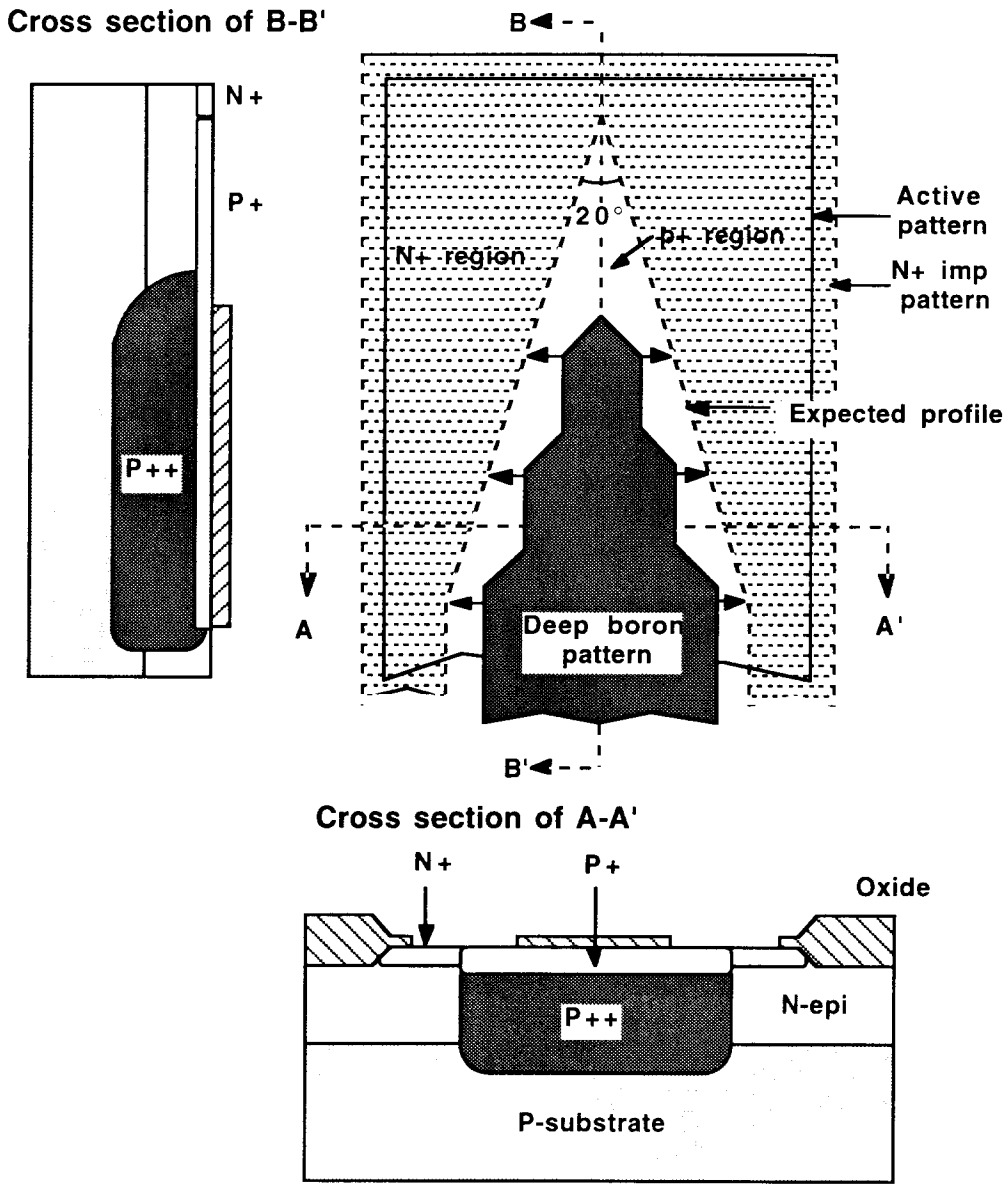

Fig. 9: Schematic diagram of the use of a shallow p-diffusion at the tip of a probe to produce greater tip sharpness.

Table 1. Simulation results of bending distance (deflection) using ANSYS*

Structure	Deflection (μm)
SiO_2/Si=2/15μm	-374.7
SiO_2/Si=1/15μm	-199.2
Si_3N_4/SiO_2/Si=0.5/2/15μm	-293.1
Si_3N_4/SiO_2/Si=0.5/1/15μm	-157.5
Si=15μm	0

*In this simulation, following parameters are assumed (negative distance (-) means that probe shank bends downwards); probe shank length=3000μm, shank width=150μm.
Internal stress (σ)=40Mpa (Si), -300Mpa (SiO_2), 950Mpa (Si_3N_4).
Young's modulus (E)=$1.7x10^5$Mpa (Si), $0.67x10^5$Mpa (SiO_2), $2.21x10^6$Mpa (Si_3N_4).

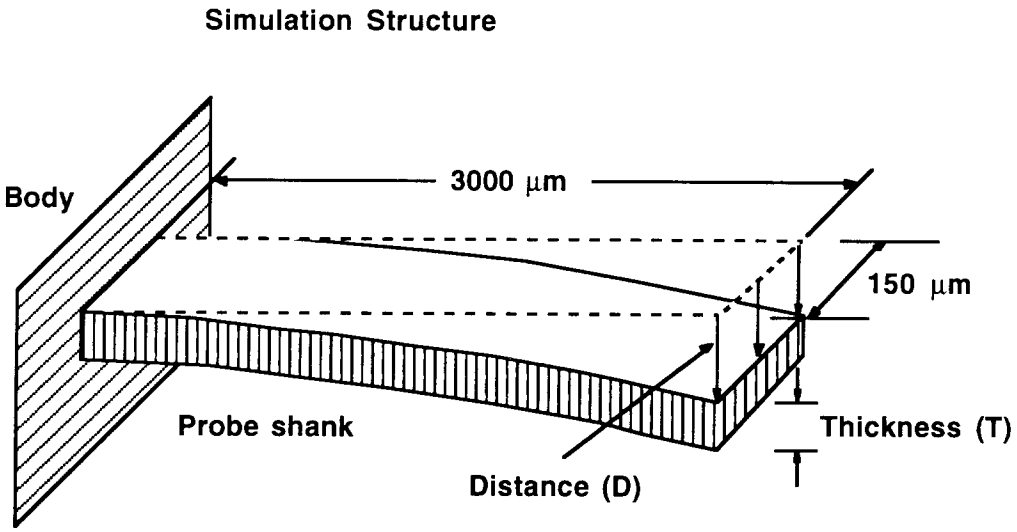

Fig. 10: Probe shank model assumed for ANSYS simulations.

STIM-2 Timing Protocol

Several communication formats for the efficient operation of the second-generation stimulating probes (STIM-2) were considered, and one of these timing protocols has now been selected. The design of a timing protocol for STIM-2 was originally based on the STIM-1 (16-bit time frame) protocol. We want to keep STIM-2 compatible with the same external interface system as that used with STIM-1, allowing only simple timing changes and requiring no significant alterations in the hardware. At the same time we want to ensure that the protocol selected is flexible enough to grow with future applications, which are expected to increase significantly in the number of sites required. In order to maintain the bandwidth of the overall system, it is desirable to keep all common operations within the present single 16-bit word frame of STIM-1. However, STIM-1 is not flexible enough as it stands to allow future expansion to larger multisite arrays without some alteration. In particular, STIM-1 lacks sufficient addressing capability for larger arrays. As a result, for

STIM-2 we have adopted the use of a single 16-bit data word for fast (frequently-used) operations, and a 32-bit data word for operations insensitive to speed.

Process technology	Modified Micromachined 3μm n-epi, p-sub, p-well CMOS process
Power voltage supplies	V_{CC}=5V, V_{SS}=-5V, Gnd=0V
Control signals	CLOCK, DATA
Current range	-127μA to +127μA
Current resolution	1μA
Power consumption	Standby ≤ 50μW, Operating ≤ 10mW
Total chip area	3844.5 x 2935.5 μm^2=11.29mm^2
Number of transistors	4706
Special modes	• built-in site activation mode • neural recording mode • ground shunt mode • anodic bias mode • current calibration mode • impedance test mode • platform address mode
Number of sites	64
No. of sites per shank	8
Number of shanks	8
Site Area	1000μm^2
Max. shank width	99μm
Shank/Site spacing	400μm

Table 2: Specifications for STIM-2: A second-generation stimulating probe.

In order to incorporate the two extra bits required to address the increased number of sites (64 versus 16) on STIM-2 in a 16-bit data frame, we have gone to an 18-clock-cycle data frame and essentially removed the strobes used in loading data from the actual bit times. This can be accomplished by minor changes (a DIP switch) in the external system and thus more actual information can be carried while using the same 16-bit data word; that is, the 16-bit word can be separated and arbitrary delays can be inserted so that the 16-bit data word can be sent in 18 actual clock cycles. In a sense, two of the bits in STIM-1 are occupied by the strobes and thus carry no real information. (STIM-1 actually uses a 14-bit word in 16 clock cycles.) In STIM-2 we will use 6 time slots (clock cycles) for addresses (addressing 64 sites), 2 time slots for modes, 8 time slots for current data, and 2 time slots for strobes. Figure 11 compares the data structures for STIM-1 and STIM-2. Modes requiring fast operation such as the recording and low-impedance shunt modes can be loaded along with routine stimulation data transfers in the 16-bit word frame, while other special modes which do not need such high speed would use a 32-bit word frame. Thus, the system bandwidth should remain high. At 4MHz, STIM-1 can load an instruction in 4μsec, whereas STIM-2 would load at 4.5μsec; however, all of the tested circuitry for STIM-1 is operational above 4MHz so the original throughput could be maintained by increasing the clock rate slightly. The additinal data word in STIM-2 will also allow expansion in the number of special modes used in future systems as well as providing expandable address space.

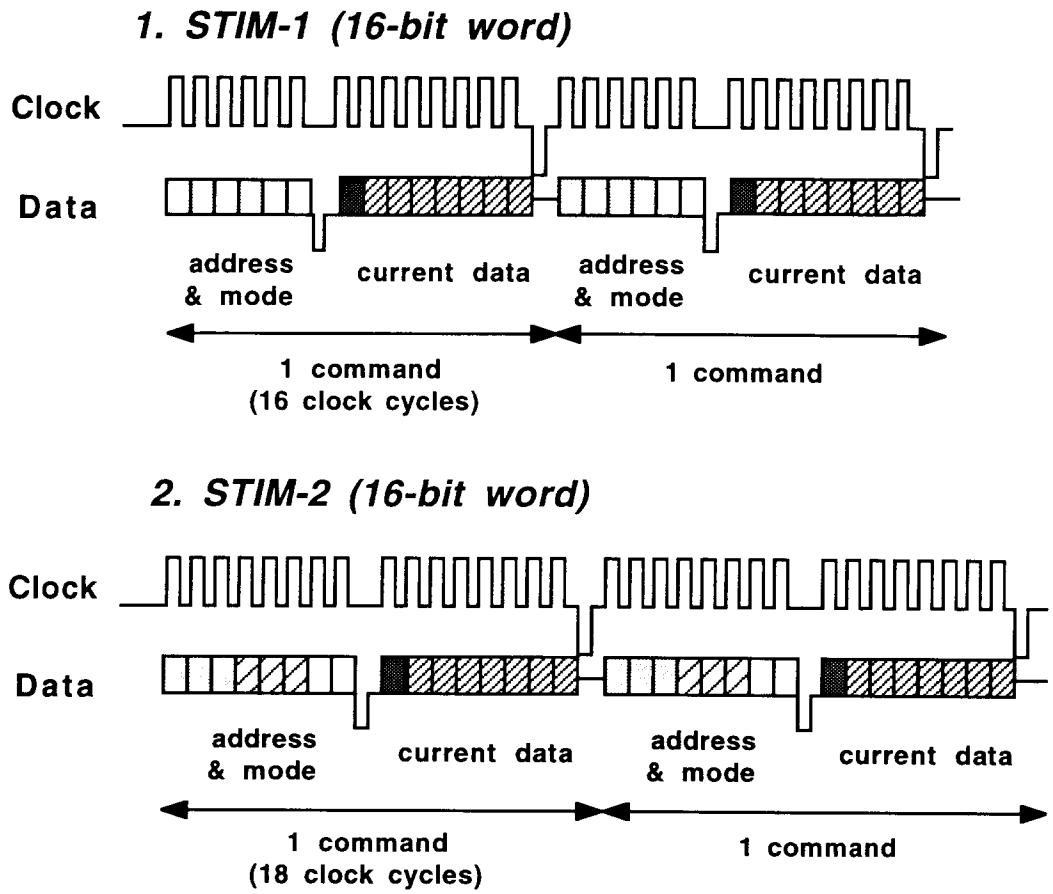

Fig. 11: Timing Comparison between STIM-1 aned STIM-2. The primary difference is that STIM-1 uses a 14-bit data word entered in 16 clock cycles; STIM-2 uses a 16-bit word entered in 18 clock cycles.

Data Designations

A more detailed view of the timing and bit designations in STIM-2 is given in Fig. 12. The upper diagram illustrates the situation when normal data are transmitted as a 16-bit word instruction. The previous 4-bit address for STIM-1 has been expanded to 6 bits to select one of 64 sites. The first and second address fields (for one-of-eight DACs, and for one-of-eight sites, respectively) are clocked in along with two mode bits, and then a strobe occurs on the data line, latching in these address and mode bits. The clock is either held up held up during this strobe or extra clock cycles are inserted here. The mode bits "00" have been arbitrary chosen as the normal stimulation mode indicator. Eight bits of current data are then clocked in. A strobe then occurs on the clock line, latching in these data, followed by the high impedance state that occurs during the last bit time, allowing the probe to transmit the "I'm OK" signal back to the external electronics. The remaining three modes are for recording (M01), low-impedance shunt (M10), and extended data word (special mode) flag (M11).

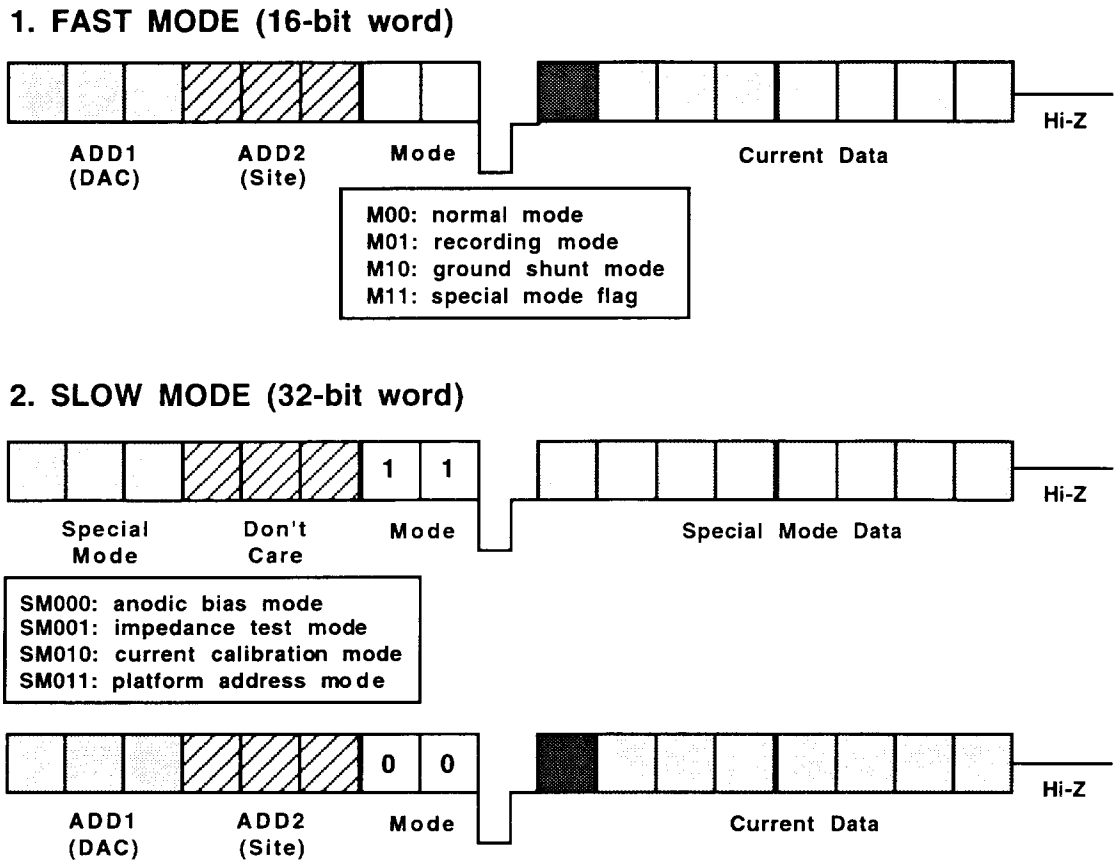

Fig. 12: Data word structures for STIM-2

The lower portion of Fig. 12 illustrates the operation of a 32-bit instruction for cases which do not require high speed operation. Once again the first and second parts of the address and the mode bits are clocked in and latched on the data strobe. At this time the mode bits are "11", indicating an extended instruction. In this case, the first three address bits in this first word are interpreted as special mode information and are latched to allow up to eight special modes. For example, at present the first four special modes are designated for anodic bias, impedance test, current calibration, and platform address as noted in Fig. 12. These mode bits are followed by three bits that for the present are *don't-care* conditions but in the future could be used for additional functions. Eight bits of special mode data follow. These could be used to address as many as 256 different probes in a distributed system, each probe having 64 sites. One special mode could be defined to allow a third data word as well, allowing the address space to be expanded further. The second 16-bit data frame is a standard probe command as used in a single instruction. Thus, for most operations on a single probe or within a 64-site address space, we need only a single 16-bit input word. However, for operations occuring rarely or not requiring high execution speed, or for switching to another address space, we would add the additional word up front. In the case of a platform, this first word would be decoded and the second word would then be passed to the selected probe. We feel that this protocol preserves compatibility with the present STIM-1 design and with its external system while

allowing plenty of room to expand the system in the future. The only real limitation is that we are constrained to a 64-site address space for single 16-bit "instructions".

Alternate Modes of Operation

In addition to the normal mode of operation (M00) used for current stimulation, there are several alternate modes whose operation will now be explained. First, in a normal data entry the two mode bits are decoded to allow three possible fast-mode operations as well as a special mode (extended instruction) flag. Each mode operates on a per-site basis affecting only the addressed site. The first mode (M00) is normal stimulation mode for current sourcing and sinking. A second mode, M01, is a recording mode in which the designated site is connected to an on-chip amplifier which allows monitoring of the neural activity near the site. In this mode, the electrode signal is recorded through an operational amplifier whose output is connected to the data pad through a transmission gate. In this configuration, the probe will remain in its present state until the next clock signal, which will release the data pad to input functions once again. If the recording channel is instead connected to a sixth output line, then monitoring could be performed continuously and indefinitely during subsequent stimulus protocols. This would seem to be a much more useful arrangement and is being considered. A sixth lead on a ribbon cable is not a significant addition. However, having the recording mode included as an option in the 16-bit frame would allow it to be performed at high speed so that it should be possible to interleave recording along with the normal stimulus changes. Thus, having the recording output connected to the data pad may not be as restrictive as it first appears.

The third mode, M10, is a low-impedance shunt mode. This feature allows the outputs of the unselected channels to be grounded if desired. A fourth mode, M11, indicates that this is the first of two data words in a 32-bit entry instruction. The special modes described below do not need to be executed at high speed and would not normally be entered frequently. Thus, the additional bits required should not greatly decrease the overall system throughput. The first special mode is an impedance test mode (SM000). During this state, a direct analog connection is made between the selected electrode and the data pad. If the DAC on that channel is set to deliver a specified current, then the voltage response can be monitored at the data pad, measuring the site impedance. Alternatively, an external signal could be applied at the pad and the impedance measured as for a normal passive electrode.

A second special mode, SM010, is the anodic bias mode. This mode biases the output of the electrode at a diode drop above ground. This helps to overcome the asymmetry of the water window around circuit ground (as defined by the hydrogen and oxygen evolution potentials). The third mode (SM011) is reserved for stimulating current calibration, both sourcing and sinking. This mode provides an analog access path from the selected DAC to the data pad, but not to both the site and data pad. The measurement of the data pad current then entirely reflects the DAC output current since there is no current path to the data pad from any of the other circuits. This mode allows DAC current calibration without stimulating the tissue. The fourth mode (SM011) extends the address space to other probes. In this mode, the internal circuitry on the presently-selected probe does not actually do anything in response to the entry word and instead waits for the next data command. This mode is useful, for example, for use with three-dimensional arrays where the platform would use the first word address to steer the subsequent word to a new probe from the array. This arrangement is similar to page-mode addressing in a memory.

Different locations on the same page/probe can be accessed rapidly, whereas external addresses take more time to execute. The remaining four modes (SM100 to SM111) are reserved for testing functions or other future features. Figure 13 illustrates each of these modes with simple diagrams.

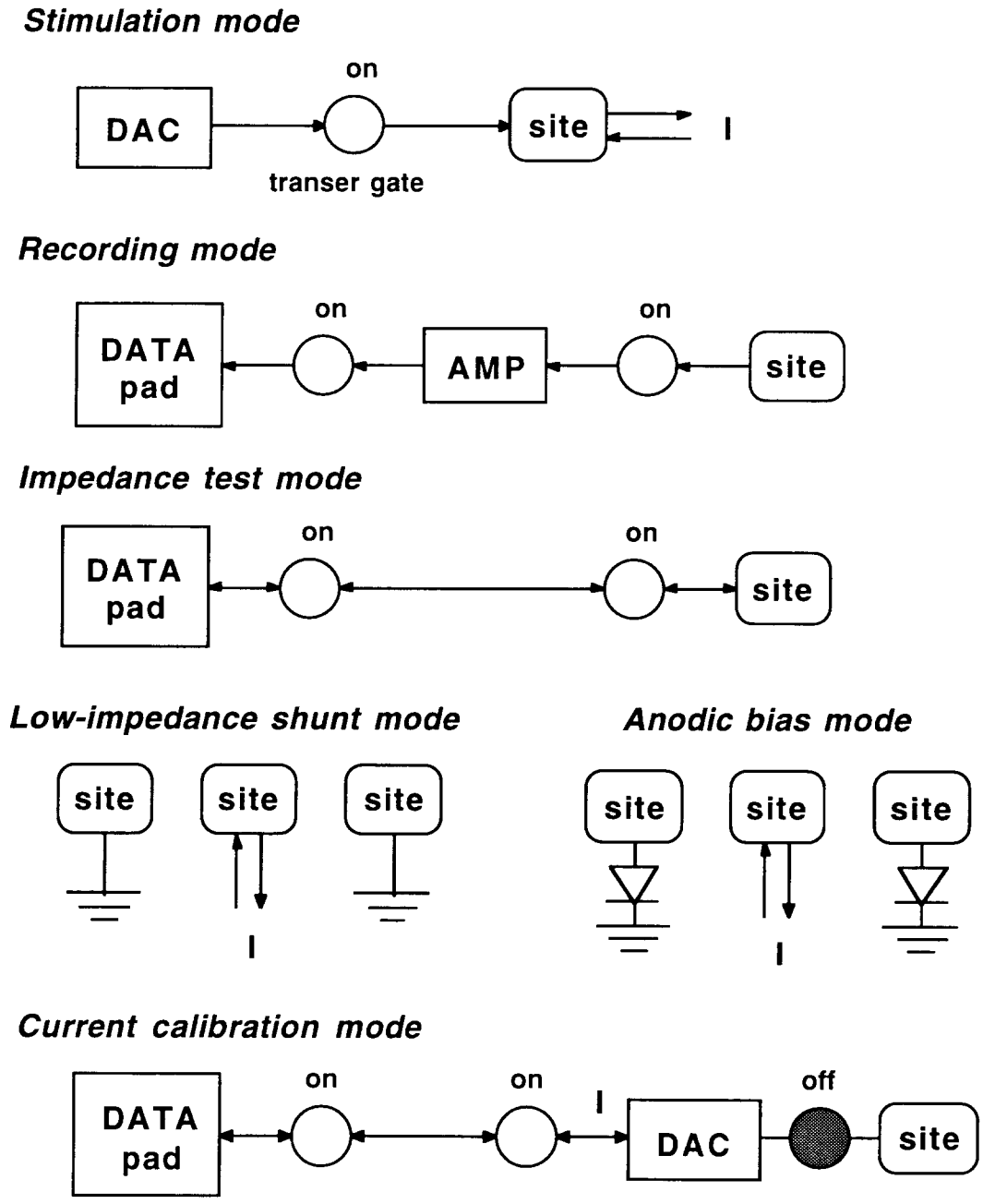

Fig. 13: Operation of the various modes on STIM-2.

On-Chip Electronics for STIM-2

Figure 14 shows the overall block diagram of STIM-2. A 16-bit word is serially clocked into the 8-bit serial shift register from the data line. The first six bits represent address, followed by the two mode bits. The first three of the address bits are decoded to select one of the eight DACs, and the second three bits are decoded to select one of the eight sites associated with that DAC for stimulation. During half of the ninth time slot, the data line sinks low to negative voltage signaling the mode and address latches to latch those bits. This strobe signal is designated as DST (data strobe). At this time the address and mode bits are decoded and latched by the AST1 and AST2 clock signals. Then, eight bits representing the amplitude and sign of the sinking or sourcing currents are directed into the level shifters, which translate them to ±5V, ensuring that the pass transistors in the DAC remain on and off completely. The selected DAC latches this current level data and delivers the corresponding current to the selected stimulating site when the clock line strobes to Vss (designated CST). This current is maintained until it is changed by external control (unless reset by its time-out circuit). Another input word can be used to initiate a current pulse on a different channel or to end the current pulse on the same channel by sending it a data word with all zeros in it for current amplitude or by simply changing the DACD (DAC disable) clock status. The clock and timing diagrams are illustrated in Figs. 15 and Fig. 16, respectively.

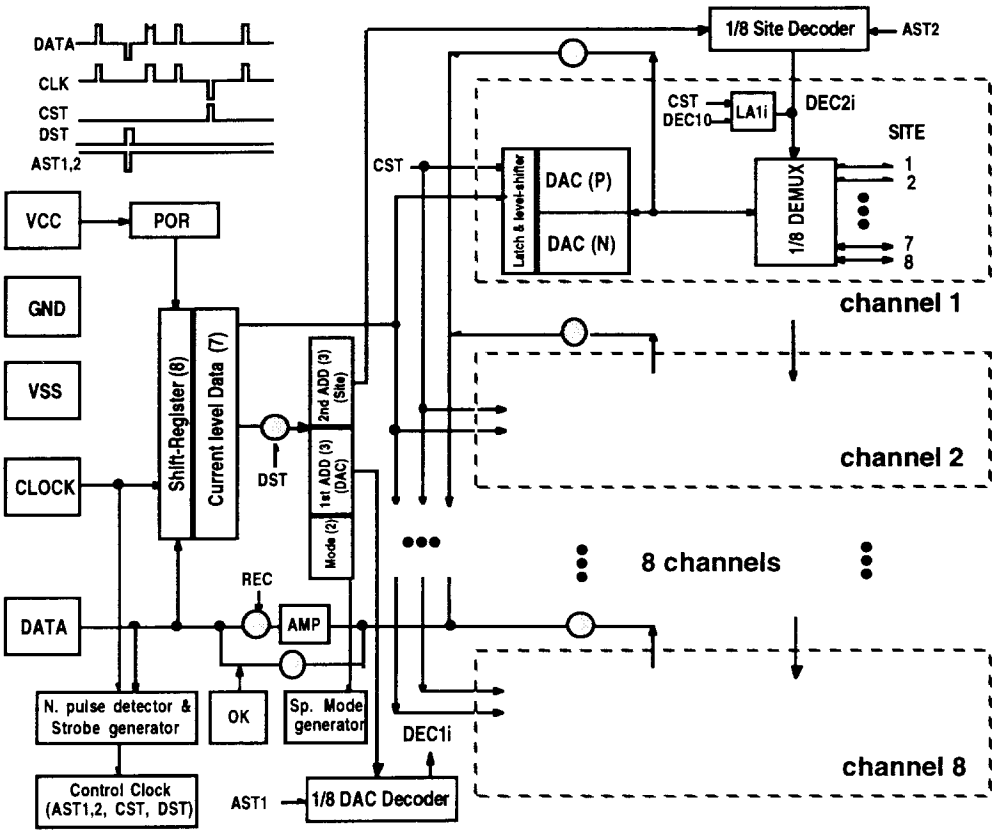

Fig. 14: Overall block diagram of STIM-2.

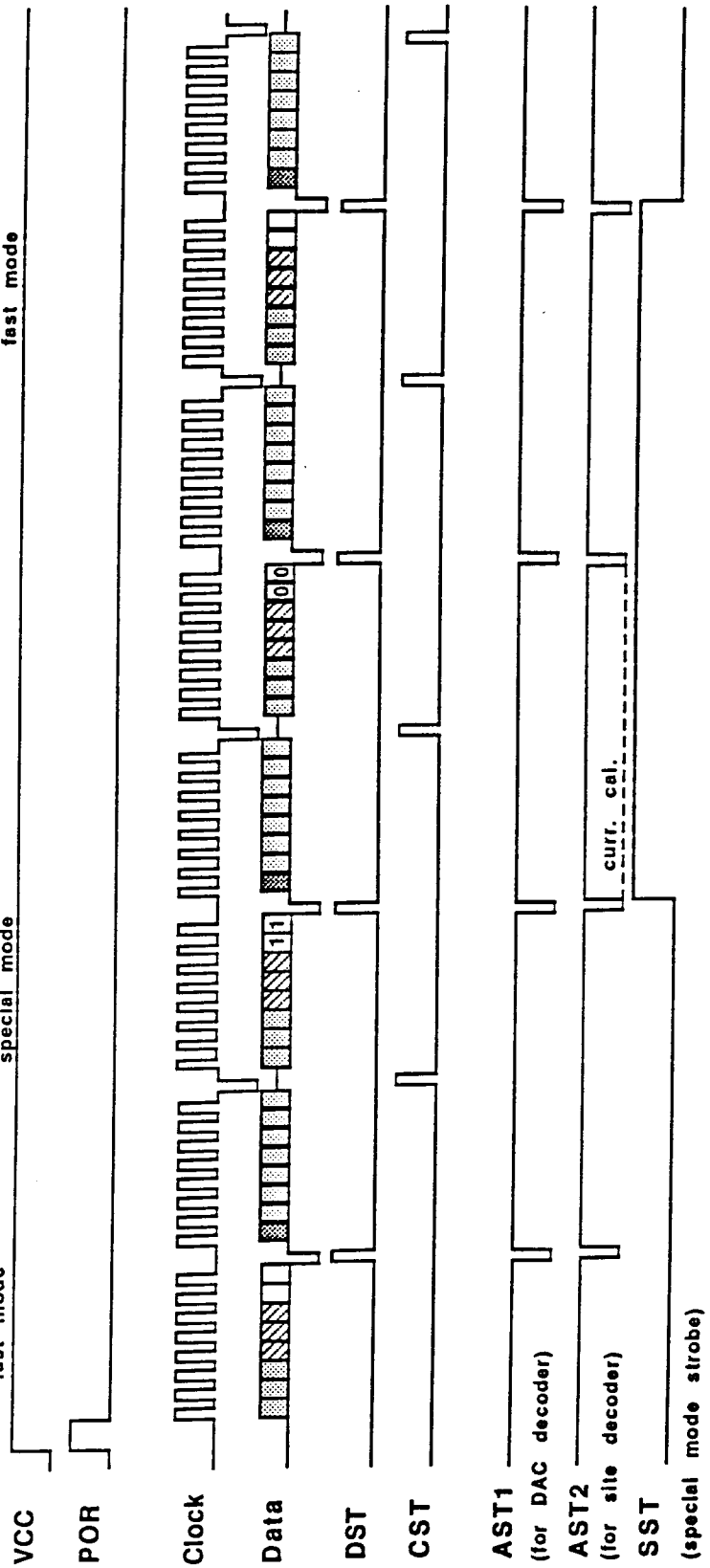

Fig. 15: Clock Diagram for STIM-2.

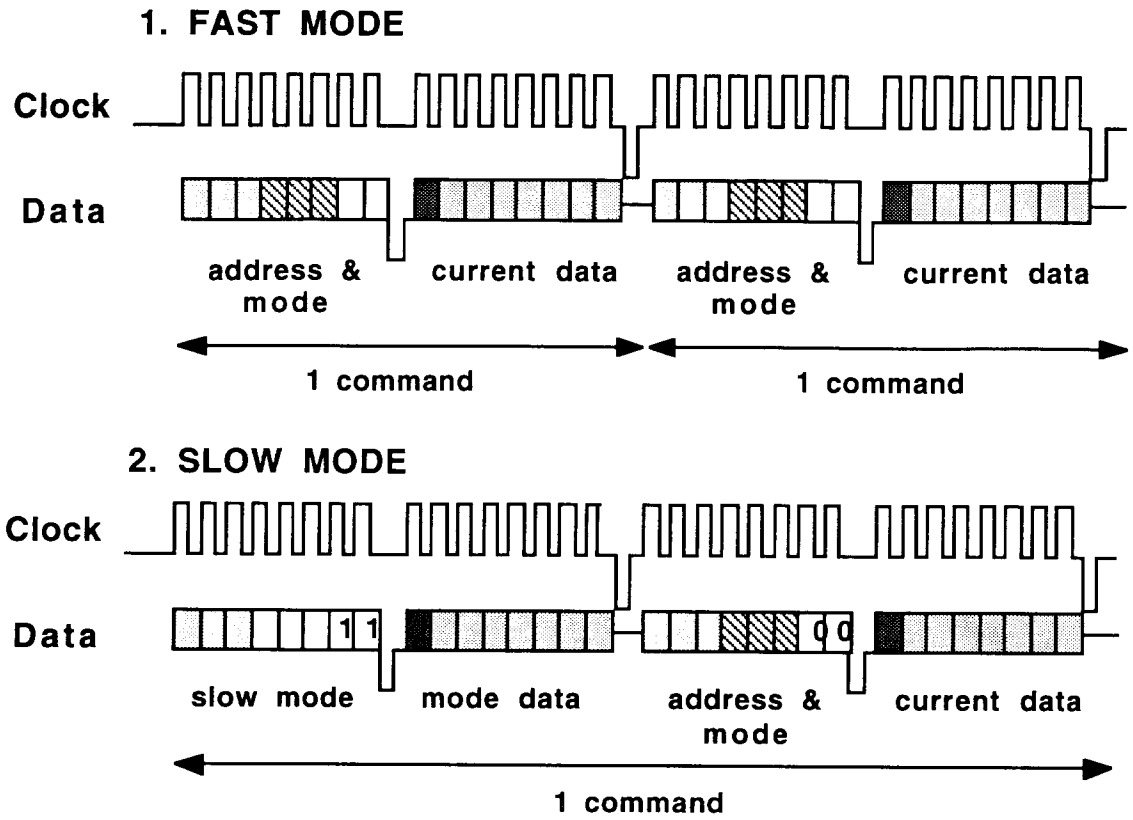

Fig. 16: Overall timing diagram for STIM-2.

The simulation data for STIM-2 will be reported in the next quarterly report. This probe is now in layout, and Fig. 17 shows a block diagram and actual layout print from these efforts. In this case, the eight-shank version of the probe is shown. This probe would be suitable for acute studies; however, the vertical extent of the circuit area above the shanks (2.9mm) is larger than desired and might lead to tissue overgrowth and anchoring to the skull in chronic applications. Accordingly, we are also exploring lower-profile layouts for the circuitry. Since in the 16-shank version the structure will be twice as wide anyway, it is appropriate to utilize this lateral area rather than extending the probe along its length. We plan to release the circuitry for fabrication at the MOSIS foundry during the coming quarter.

5. Stimulation System External Electronics

During the past quarter, the external electronics for stimulation probes has been enhanced in two ways. First, one of the proposed improvements in the binary to ternary conversion electronics mentioned briefly in the last quarterly report under the previous contract has been implemented. Second, work has gone forward on the DSP program in the external electronics.

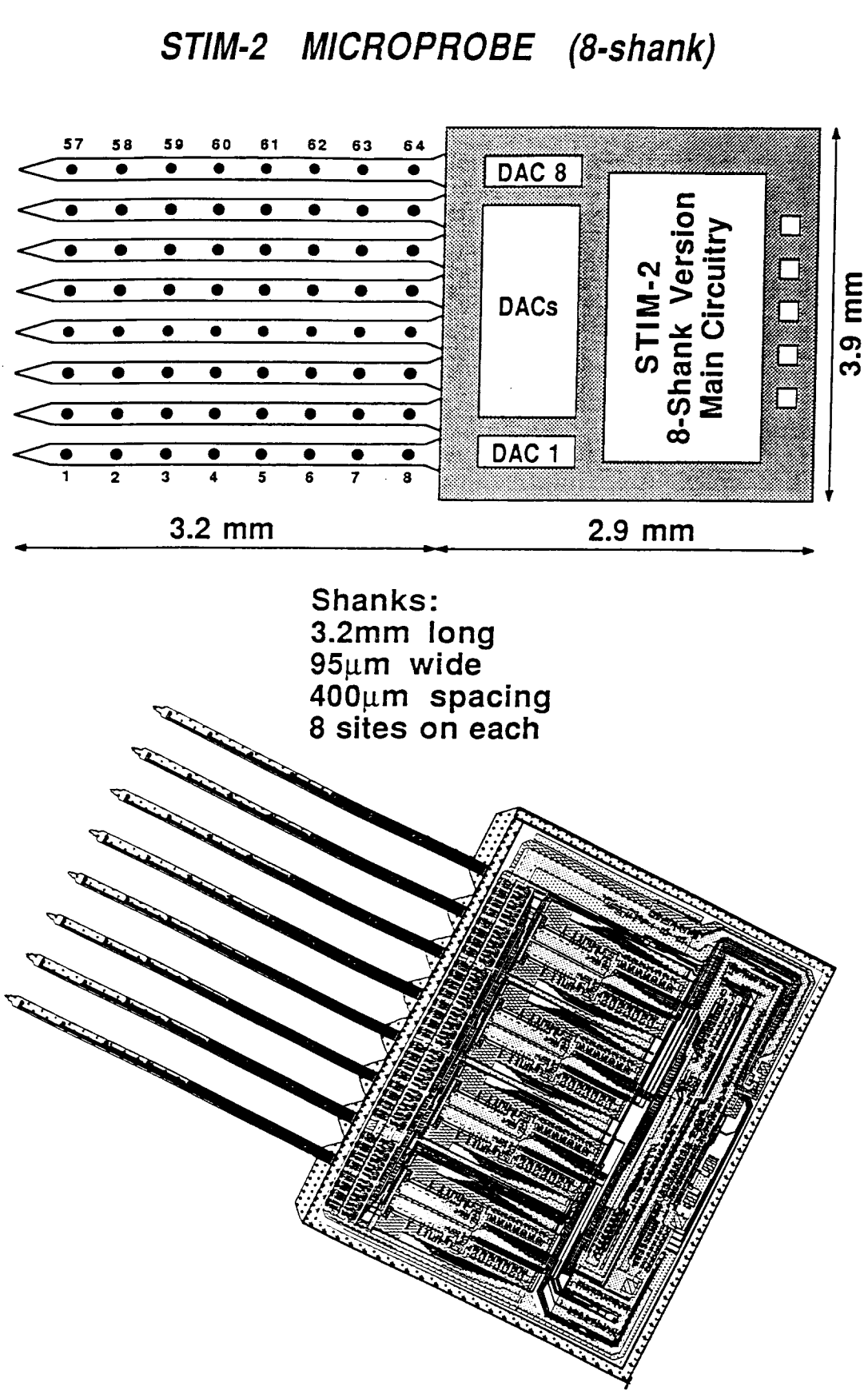

Fig. 17: Block diagram and initial layout of STIM-2.

As described in previous reports, the original design of the binary to ternary conversion circuitry in the external electronics was found to have some problems. The conversion started with two binary streams, one containing positive pulse information and one containing negative pulse information. The negative pulse stream was passed through an inverting opamp, and then summed with the positive pulse stream using another opamp. Extremely fast opamps were required, with slew rates over 400V/μsec, and the high gain involved caused severe ringing at the output. This was very sensitive to circuit parasitic capacitance, and since the second opamp output directly fed the stimulation probes, these capacitances could vary with probe positioning, lead length, and so forth.

It was previously proposed to explore the use of switching transistors or multiplexers to get away from the problems which linear circuitry such as opamps caused. Two solutions have been tried, with the second one producing a very satisfactory result which will probably be utilized in building the final version of the remote converter. Both of the solutions tried involved the use of analog switches. The first used a 4:1 analog multiplexer with a built-in decoder. The four multiplexed inputs were +V, GND, -V, and the fault detection circuitry for the high-impedance state. The two decoder selection inputs were connected to the positive and negative binary stream lines. The +V state was selected by the positive stream being active and the negative inactive. The -V state was selected by the negative stream being active and the positive inactive. The GND state was selected by both being inactive. Finally, the high-impedance state was selected by both lines being active at once. This circuit turned out to be fast enough, but there were problems with decoding glitches. This could generate a negative spike at the output during a transition from the ground to the high-impedance state, for example, which the probe would see as a latching strobe at an inappropriate time.

In general, decoding glitches are inherent to asynchronous logic, and the solution to a no-glitch requirement is to use synchronous logic. This solution would have complicated the overall circuit considerably, however. Instead, it was decided to try and find a way to glitchlessly decode with asynchronous logic. This turned out to be possible if the high-impedance state information was supplied by a third, separate binary line. This was easy to implement, because that was how the high-impedance state was controlled in the original opamp circuit.

The conversion circuit employed is shown in Fig. 18. In this circuit, the + binary line directly controls the +V analog switch, and the - binary line the -V switch. Thus the +V and -V outputs can ONLY be enabled if the respective control lines are active. The ground state is enabled by the NOR of the two binary control lines. Due to the finite turn-on and turn-off times of the switches, it is possible to have both the positive and negative switch on at the same time during a transition from +V to -V or vice versa. This is analogous to what happens when CMOS logic makes a transition. The 200Ω resistors, combined with the 30-50Ω on-resistance of the switches themselves, limit the current flow during the few nanoseconds for which this is possible to around 20mA for the case where +V and -V are +5 and -5, respectively. During such a transition, the two resistors involved act as a voltage divider, presenting 0 volts at the combined output, which is a desirable transitional result. The high-impedance state is achieved by a separate analog switch which is in series with the combined output of the first three.

This circuit has the additional advantage over the opamp solution of providing much more convenient control of the voltages of the ternary output. The output current of the

DACs on the STIM chips are calibrated by adjusting the +V supply to the STIM chip. The swings of the ternary data and clock lines must be adjusted to match. With the former opamp circuit, the +V value was adjusted by trimming the feedback resistor that sets the opamp gain. In the new circuit, the adjusted power supply voltage that is fed to the STIM chip is simply directly connected to the +V inputs of the analog switches, and the data and clock line voltages track automatically, with no secondary adjustment step as with the opamp resistor.

Now that a robust solution to binary to ternary conversion has been achieved, the overall circuit for the remote converter can be finalized, and a permanent wirewrap circuit built to replace the breadboard that the remote converter development has been done on.

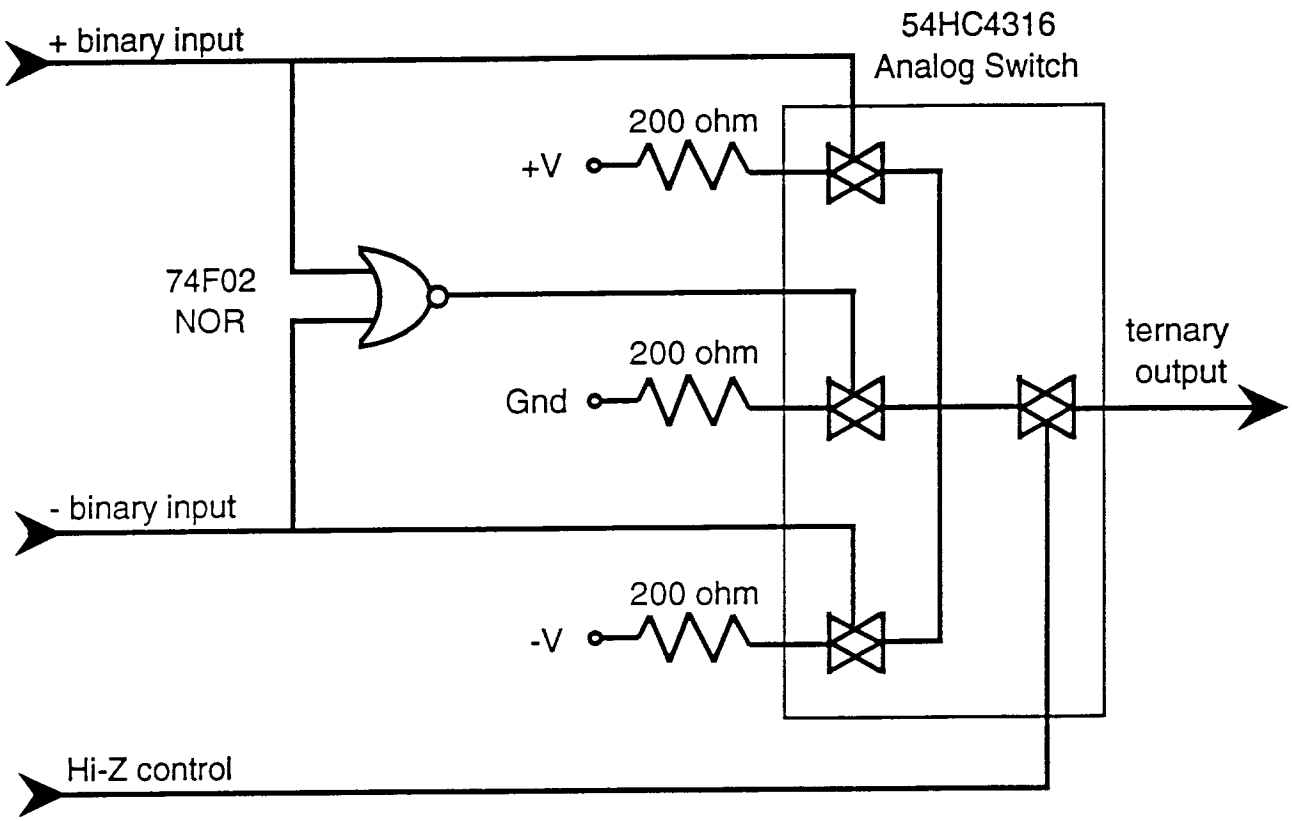

Fig. 18: The binary to ternary converter developed for active multichannel probes using high-impedance control.

Work has been started on converting the software supporting the external electronics from a form suitable for testing probes to a form more suitable for doing stimulation experiments. The purpose of the DSP board in the external electronics was to provide an engine which could generate stimulation data at the 4 Mbit/second bandwidth required for sustained periods of time. For probe testing purposes, however, it was only necessary to produce streams at this rate for short bursts. This was achievable without the use of the DSP chip by putting the external electronics daughter board in a halt state, loading the daughter board FIFO with up to 1 K words of data, and then putting the board in a run state. The original software was designed to have the host computer, which is

much slower than the DSP, write THROUGH the DSP board to the daughter board to load the FIFO, since the bandwidth was not critical while the daughter board was in the halt state. A program running on the DSP board was not necessary using this approach, but only 1K-word worth of data could be delivered at maximum data rate by this method.

In anticipation of more extensive testing and actual stimulation experiments, the development of a TMS 320C25 DSP program has been started. The initial phase which has been completed is to write a simple DSP program which accepts data from the host computer program and passes it through to the daughter board. This program interprets commands telling it to pass data to the daughter board control register or FIFO, followed by the appropriate data.

Having completed this initial DSP program, it has become apparent that further information is needed to proceed from here. The questions that need to be answered concern just what type of stimulation sequences are required for real stimulation experiments. Can all of the required events be held in the memory of the DSP board, or will it be necessary for the DSP board to do calculations in order to extend and modify sequences on the fly? The answer to this question dictates the complexity of the DSP programs required and is dependent upon the complexity and length of the stimulation sequences required. Further development of this program awaits the answers to such questions, which are being explored.

6. Conclusions

During the past quarter, research performed under this program has focused on four primary areas. Passive probes have been fabricated having multiple shanks and site areas ranging from 400μm^2 to 1600μm^2 so that the problems associated with tissue access resistance and the physiological effects of stimulation can be studied chronically. A series of passive probes is also being designed to allow different tip shapes to be created so that the tips can be optimized to obtain minimum insertion force and minimum tissue damage. A combined stimulation-recording probe is also in development that should allow questions regarding the fall-off of spike amplitudes observed with chronic recording electrodes after 8-10 months in-vivo to be answered.

While the new process for active probes has produced good results and appears to have solved the former processing problems associated with circuit interconnect and encapsulation, several minor problems still needing correction have been identified. The perimeter of these probes needs to be expanded near the outer corners of the circuit area to prevent undercutting during the silicon etch used to separate the probes from the wafer; processes have also been identified for further sharpening the probe tips using a shallow boron diffusion to extend the substrate beyond that produced using the deep etch-stop diffusion. In addition, experiments to better characterize appropriate dielectric thicknesses on the probes to prevent bowing have been carried out. This reoptimization has been motivated by the retention of low-temperature oxide (LTO) on the shanks of some of our recent probes. Finally, low-voltage leakage has been seen on the recently-fabricated active stimulating probes. We suspect this may be due to punchthrough of the epitaxial region. Studies are underway to confirm this cause, in which case the epitaxial layer thickness will be increased somewhat on future fabrication runs.

The design of the circuitry for a second-generation active probe, STIM-2, was completed during the past term. This probe will be implemented in 8- and 16-shank versions and will feature eight parallel channels. Per-channel currents will be controlled within 1μA over a range from 0 to ±127μA. A front-end selector will interface eight DACs with 8 sites from among 64 present on the probe, thus allowing precise positioning of the active sites in tissue. The timing and data protocols developed for STIM-2 allow all modes developed for STIM-1 to be retained. In addition, additional modes such as the ability to record from any site have been added. The circuitry allows direct addressing of up to 64 sites with a single 16-bit data word and using a second 16-bit word allows up to 256 such probes to be addressed. Hence, normal operations on a single probe can be carried out using single 16-bit instructions with a 4μsec time period between changes in probe state using a 4.5MHz clock. Switching between probes as well as the implementation of modes insensitive to speed (e.g., current calibration, site testing) use the slower 32-bit instructions. Progress has also been made with the external system for use with these active probes in both the hardware and software areas. This system will be used in the further testing of both STIM-1 and STIM-2.

During the coming quarter, we hope to begin a series of chronic stimulation experiments to explore the effects of stimulation on the tissue. We also hope to complete the development of the electrodes needed for the penetration studies. The testing of STIM-1 should be completed along with any appropriate design optimizations. Finally, we hope to receive MOSIS chips back with the circuitry for STIM-2 so that this circuitry can be tested to establish design validity. Following that, a new fabrication run of both STIM-1 and STIM-2 will be initiated.